Radiotherapy and Oncology 136 (2019) 98–105

Contents lists available at ScienceDirect

Radiotherapy and Oncology

journal homepage: www.thegreenjournal.com

Original Article

Comparison of hyper- and hypofractionated radiation schemes with IMRT technique in small cell lung cancer: Clinical outcomes and the introduction of extended LQ and TCP models

Qi-Wen Li [a,1], Bo Qiu [a,1], Bin Wang [a,1], Jun Zhang [a], Li Chen [a], Yin Zhou [b], Jun-Kun Qin [c], Su-Ping Guo [a], Wei-Hao Xie [a], Zhou-Guang Hui [d], Ying Liang [e], Jin-Yu Guo [a], He Wang [f], Meng Zhu [f], Wen-Tong Shen [g], Long-Yan Duan [g], Li-Kun Chen [e], Li Zhang [e], Hao Long [h], Yi-Ming Wang [i,*], Hui Liu [a,*]

[a] *Department of Radiation Oncology, State Key Laboratory of Oncology in South China, Collaborative Innovation Center for Cancer Medicine, Sun Yat-sen University Cancer Center, Guangzhou;* [b] *Evidance Medical Technologies Inc., Suzhou;* [c] *Zhixin High School, Guangzhou;* [d] *Department of Radiation Oncology, National Cancer Center/Cancer Hospital, Chinese Academy of Medical Sciences and Peking Union Medical College, Beijing;* [e] *Department of Medical Oncology, State Key Laboratory of Oncology in South China, Collaborative Innovation Center for Cancer Medicine, Sun Yat-sen University Cancer Center, Guangzhou;* [f] *Homology Medical Technologies Inc., Suzhou;* [g] *Department of Radiation Oncology, Ruijin Hospital, Shanghai Jiaotong University School of Medicine, Shanghai;* [h] *Department of Thoracic Surgery, State Key Laboratory of Oncology in South China, Collaborative Innovation Center for Cancer Medicine, Sun Yat-sen University Cancer Center; and* [i] *Department of Oncology, The First Affiliated Hospital of Jinan University, Guangzhou, China*

ARTICLE INFO

Article history:
Received 3 September 2018
Received in revised form 27 March 2019
Accepted 31 March 2019
Available online 15 April 2019

Keywords:
Small cell lung cancer
Hypofractionated radiotherapy
Tumor control probability
LQ model
4Rs

ABSTRACT

Purpose: To evaluate the outcomes of 45 Gy/15 fractions/once-daily and 45 Gy/30 fractions/twice-daily radiation schemes utilizing intensity-modulated radiation therapy (IMRT) in extensive stage small cell lung cancer (SCLC), and to build up a new radiobiological model for tumor control probability (TCP) considering multiple biological effects.

Methods: Fifty-eight consecutive patients diagnosed with extensive stage SCLC, treated with chemotherapy and chest irradiation, were retrospectively reviewed. Thirty-seven received hyperfractionated IMRT (Hyper-IMRT, 45 Gy/30 fractions/twice-daily) and 21 received hypofractionated IMRT (Hypo-IMRT, 45 Gy/15 fractions/once-daily). Local progression-free survival (LPFS) and overall survival (OS) were calculated and compared. An extended linear-quadratic (LQ) model, LQRG, incorporating cell repair, redistribution, reoxygenation, regrowth and Gompertzian tumor growth was created based on the clinical data. The TCP model was reformulated to predict LPFS. The classical LQ and TCP models were compared with the new models. Akaike information criterion (AIC) was used to assess the quality of the models.

Results: The 2-year LPFS (34.1% *vs* 27.9%, $p = 0.44$) and OS (76.9% *vs* 76.9%, $p = 0.26$) were similar between Hyper- and Hypo-IMRT patients. According to the LQRG model, the α/β calculated was 9.2 (95% confidence interval: 8.7–9.9) Gy after optimization. The average absolute and relative fitting errors for LPFS were 9.1% and 18.7% for Hyper-IMRT, and 8.8% and 16.2% for Hypo-IMRT of the new TCP model, compared with 29.1% and 62.3% for Hyper-IMRT, and 30.7% and 65.3% for Hypo-IMRT of the classical model.

Conclusions: Hypo- and Hyper-IMRT resulted in comparable local control in the chest irradiation of extensive stage SCLC. The LQRG model has better performance in predicting the TCP (or LPFS) of the two schemes.

Abbreviations: IMRT, intensity-modulated radiation therapy; SCLC, small cell lung cancer; TCP, tumor control probability; Hyper-IMRT, hyperfractionated intensity-modulated radiation therapy; Hypo-IMRT, hypofractionated intensity-modulated radiation therapy; LPFS, local progression-free survival; OS, overall survival; BED, biological effective dose; CT, computed tomography; LQ, linear-quadratic; LQRG, linear-quadratic model incorporating cell repair, redistribution, reoxygenation, regrowth and Gompertzian tumor growth; AIC, Akaike information criterion; MRI, magnetic resonance imaging; PET, positron emission tomography; CR, complete remission; PR, partial remission; GTV, gross tumor volume; CTV, clinical target volume; PTV, planning target volume; Dmax, maximum dose; RECIST, Response Evaluation Criteria in Solid Tumors; CTCAE, Common Terminology Criteria Adverse Events; DVH, dose–volume histogram; SF, surviving fraction; MAE, mean absolute error; MRE, mean relative error; LQG, Linear Quadratic model with Gompertzian tumor growth.

* Corresponding authors at: Department of Radiation Oncology, Sun Yat-sen University Cancer Center, No.651 Dongfeng Road East, Guangzhou 510060, China (H. Liu).
E-mail address: liuhui@sysucc.org.cn (H. Liu).

[1] Qi-Wen Li, Bo Qiu and Bin Wang contributed equally to this work.

https://doi.org/10.1016/j.radonc.2019.03.035
0167-8140/

Small cell lung cancer (SCLC) is characterized by rapid growth. Shortening radiation time may be effective in avoiding accelerated repopulation and improving clinical outcomes [1]. Turrisi et al. performed the first phase 3 clinical trial comparing two schedules, 45 Gy/30 fractions/twice-daily and 45 Gy/25 fractions/once-daily in limited stage SCLC, and demonstrated a significant survival benefit from the former schedule [2]. The dose split is believed to protect the late response tissues, which is characterized by low α/β and therefore especially sensitive to the magnitude of the dose per fraction. However, the twice-daily scheme is questioned due to the high incidence of acute esophagitis and its practical inconvenience.

One of the ways to compress overall treatment time is to employ hypofractionated radiotherapy. Intensity-modulated radiation therapy (IMRT) has now replaced the conventional planning technique and has demonstrated superior sparing of normal tissues [3,4]. Improvements in set-up techniques and cone-beam computed tomography (CT) scan improve the precision of treatment delivery [5]. It becomes possible to deliver the one-day dose in a single fraction without overexposure of normal tissues. Safe delivery of moderately hypofractionated schemes, e.g. 42 Gy/15 fractions/once-daily and 55 Gy/22 fractions/once-daily [6,7], has been reported. Because a survival benefit of chest irradiation in extensive stage SCLC has been documented [8], it is justifiable to compare different radiation schemes in these patients.

Another question is whether the classical linear-quadratic (LQ) and tumor control probability (TCP) models are still appropriate in predicting tumor response in SCLC. The LQ model provides the theoretical background for estimating TCP via the calculation of biological effective dose (BED) [9–11]. However, results of the CONVERT study [12] yielded statistically comparable local progression-free survival rates between 45 Gy/30 fractions/twice-daily and 66 Gy/33 fractions/once-daily schemes, although BED in the once-daily group was significantly higher. It indicated that these models need to be validated and updated with clinical data, rather than be only based on simplified assumptions and in-vitro data.

To improve the classical radiobiological models, a number of works have been performed. Repopulation used to be included in the LQ model in a very simple form based on the assumption of a time-dependent exponential term factored into the predicted clonogenic survival [13,14]. To add more features, some researchers attempted to employ a time delay for the repopulation [13,14], a Gompertzian model for tumor growth [15–19], or to incorporate redistribution and re-oxygenation into the model [20–22]. Others tried to provide more clinically relevant TCP modeling, which succeeded in predicting tumor response to stereotactic body radiation therapy in non-SCLC [19,23]. However, little work has been done to incorporate simultaneously these improvements in the fitting of local progression-free survival (LPFS) in the radiation of SCLC.

We designed a retrospective study assessing the efficacies and toxicities between two different IMRT radiation schemes, 45 Gy/30 fractions/twice-daily (Hyper-IMRT) and 45 Gy/15 - fractions/once-daily (Hypo-IMRT), in extensive stage SCLC. An extended LQ model, LQRG, incorporating all the four "R"s of radiobiology and more realistic assumptions for the prediction of TCP, was created to account for the LPFS.

Materials and methods

Study population

The study was reviewed and approved by Ethics Committee of Sun Yat-sen University Cancer Center. Since it was a retrospective study, a waiver of informed consent was granted.

From March 2010 to September 2016, fifty-eight consecutive patients treated in our institute were retrospectively reviewed. They were (1) pathologically confirmed with SCLC; (2) clinically diagnosed as extensive stage according to Veterans Administration Lung Cancer Study Group staging, based on medical history, physical examination, chest and upper abdomen CT, brain magnetic resonance imaging (MRI) and bone scan, with or without whole body positron emission tomography (PET)/CT; (3) achieving complete remission (CR) of the distant disease, and CR or partial remission (PR) in the chest after chemotherapy; (4) treated with chest IMRT with the scheme of either 45 Gy/30 fractions/twice-daily or 45 Gy/15 fractions/once-daily; (5) having regular radiological follow-up. Patients lost to follow-up within two months after radiation were excluded.

Treatments

Patients received either concurrent or sequential chemotherapy, with etoposide and cisplatin administered every three weeks for 4–6 cycles.

In the delivery of radiation, patients were immobilized in a vacuum pad in the supine position, and then scanned with the CT slice thickness of 5 mm. The gross tumor volume (GTV) was contoured restricted to traceable primary tumor and positive lymph nodes. The clinical target volume (CTV) was delineated to cover 6 mm surrounding the GTV and involved node regions. An expansion of 5 mm of the CTV created planning target volume (PTV). Either 45 Gy/30 fractions/twice-daily or 45 Gy/15 fractions/once-daily was prescribed depending on the preference of the individual radiation oncologist. At least 95% of PTV received 95% of prescription dose. The dose constraints on the organs at risk were: V20 <30% for lungs; mean lung dose <19 Gy; maximum dose (Dmax) of esophagus <50 Gy; Dmax of spinal cord <32 Gy; V30 <30% for heart for the Hyper-IMRT. For the Hypo-IMRT, V20 <28% for lungs; mean lung dose <18 Gy; Dmax of esophagus <48 Gy; Dmax of spinal cord <30 Gy; V30 <28% for heart. An IMRT technique was applied when planning the treatment.

Follow-up

Patients were first followed up two months after the completion of treatment, every three months in the first two years, and every six to twelve months thereafter. History taking, physical examination, chest and upper abdomen CT, and brain MRI were performed routinely. Bone scan, PET/CT, endoscopy or biopsy was performed if necessary. Tumor response was evaluated by Response Evaluation Criteria in Solid Tumors (RECIST) version 1.1. The immediate response was determined according to workups at the first follow-up. Local recurrence was defined as relapse within the ipsilateral hemithorax, mediastinum or/and upper clavicle fossa. Time from the start of chest radiotherapy to first local progression or death from any cause was calculated as LPFS and overall survival (OS). Toxicities occurring during radiation or within one month after radiotherapy were recorded, except for radiation pneumonitis, which was documented until one year after radiation. Toxicities were evaluated by Common Terminology Criteria Adverse Events (CTCAE) version 3.0 [24].

Statistical methods

Fisher's exact test was performed to compare the distribution of clinico-pathologic parameters. The Kaplan–Meier method was used to estimate the LPFS and OS, which were compared by the log-rank test. Cox proportional hazards modeling was used for univariate analysis. A p value (both sides) <0.05 was considered

as statistically significant. Statistics were performed by SPSS 21.0 (IBM Corp, Armonk, USA).

Tumor control probability modeling

The construction of classical LQ model combined with a Binomial TCP model, and the LQRG model combined with a Gaussian TCP model are detailed below.

(1) The classical LQ and TCP models

The surviving fraction (SF) of clonogenic cells is expressed as:

$$SF(t) = \exp\left(-\alpha D - \beta D d + \frac{\ln 2(T + \Gamma - T_k)}{\tau_P}\right) \quad (1)$$

where the parameters α and β represent lethal lesions made by one- or two-track actions, respectively; D is the total dose; d is the fractional dose; τ_P is the tumor doubling time; T is the treatment time; T_k is the delayed time for regrowth; Γ is the elapsed time since the end of treatment. $t = T + \Gamma$ is the time from the start of radiotherapy to the time of follow up. The BED is expressed as [25]:

$$BED = D + \frac{\beta D d}{\alpha} - \frac{\ln 2(T - T_k)}{\alpha \tau_P} \quad (2)$$

The TCP is defined as the probability of killing all the clonogenic cells at time t:

$$TCP(t) = (1 - SF(t))^{K_0} \quad (3)$$

where K_0 is the initial average number of clonogenic cells.

$$K_0 = V_0 \rho \quad (4)$$

where V_0 is the initial average tumor volume; ρ is the number of tumor cells in a unit volume.

(2) The LQRG and TCP models

The LQRG and its TCP model account for the four "R"s effects, and add features of delayed regrowth [13] and Gompertzian tumor growth [15,23]. The model name "LQRG" stands for the Linear Quadratic model with four "R" effects and Gompertzian tumor growth. As clinically relevant tumor local control model, they are based on three assumptions [23]:

1) the tumor would be controlled for an individual patient if the number of tumor cells K is smaller than a critical number K_{cr}, i.e., the local control probability for a tumor with K tumor cells is given by a step function:

$$P(K, K_{cr}) = \begin{cases} 0 & K > K_{cr} \\ 1 & K < K_{cr} \end{cases} \quad (5)$$

2) the distribution of K follows a Gaussian distribution for the patient population with a mean value of $\bar{K}$

$$K = \frac{1}{\sqrt{2\pi}\sigma_k} e^{-\frac{(k-\bar{k})^2}{2\sigma_k}} \quad (6)$$

3) the regression of $\bar{K}$ can be described by the following expression $\bar{K} = K_0 \cdot SF$. Following this tumor control model and the derivation from the study of Tai et al. [23], the TCP is:

$$\mathrm{TCP}(t) = 1 - \frac{1}{\sqrt{2\pi}} \int_{-\infty}^{x_0} \exp\left(-\frac{x^2}{2}\right) dx \quad (7)$$

with

$$x_0 = \frac{\bar{K} - K_{cr}}{\sigma_k} = \frac{SF - K_{cr}/K_0}{\sigma_k/K_0} \quad (8)$$

where σ_k is the Gaussian width for the distribution of tumor cell numbers.

The SF in the above formulas is expressed as:

$$SF(t) = \exp\left(-\alpha D - \beta G(\tau_R) D^2 + \left(\frac{1}{2}\sigma^2\right) G(\tau_S) D^2 + \ln 2 \frac{T - T_k}{\tau_P} + \left(\ln 2 \frac{\Gamma}{\tau_P}\right)^{\delta}\right) \quad (9)$$

where $G(\tau)$ is the generalized Lea–Catcheside function [11,26], defined by (Eq. 10); τ_R is the average DNA repair time; τ_S is average resensitization time; σ is the variance of the Gaussian distribution of random variable α, immediately after an acute irradiation; T is the treatment time; T_k is the delayed time for regrowth; Γ is the elapsed time since the end of treatment. $t = T + \Gamma$, is the time from the start of radiotherapy to the time of follow up. The first and second terms describe cell killing by one-track and two-track action (and possible repair), respectively. The third term refers to intercellular diversity of radiosensitivity and resensitization [20]. The forth term refers to the delayed tumor regrowth, while the last term involving parameter δ refers the Gompertzian tumor growth after radiation [27]. Although quite different phenomena, redistribution and reoxygenation do share a common outcome [28], a postirradiation increase in the sensitivity of cells that survive an initial or partial exposure. Following Brenner et al. [20], we denote this common outcome *resensitization* and incorporates these two "R"s in the third term of the exponent of SF. The generalized Lea–Catcheside function in (Eq. 9) is originally derived as a factor of the second term $-\beta G(\tau_R) D^2$ to describe the DNA damage corresponding to the misrepair of repairable damage. It describes the effect of radiation on the DNA repair which occurs during irradiation or between dose fractions. Following the derivation in previous studies [11,26], it takes the form of

$$G(\tau) = \left(\frac{2}{D^2}\right) \int_0^{\mathrm{T}} R(u) du \int_0^{u} R(w) \exp\left(-\frac{u - w}{\tau}\right) dw \quad (10)$$

where the function $R(t)$ describes the variation in dose rate as a function of time over the entire course of the treatment. For regular irradiation $G = 1$, but for prolonged irradiation $G < 1$ since the kernel $\exp[-(u - w)/\tau] \leq 1$ for $w \leq u$. The generalized Lea–Catcheside function is also included in the third term $\left(\frac{1}{2}\sigma^2\right) G(\tau_S) D^2$ to describe the effect of radiation on the intercellular diversity of radiosensitivity and resensitization occurring during irradiation or between fractions [20]. The opposite sign of the second and third term implies the opposite contribution to the SF, while the time constant in the two generalized Lea–Catcheside functions have different meanings: one for the average DNA repair time, and the other for the average resensitization time. The generalized Lea–Catcheside function, also called the Lea–Catcheside dose-protraction factor [29], is uniquely dependent on the temporal behavior of radiation delivery in its entirety. When the cumulative doses D for the two treatment schemes are the same, it is the only essential element contributing to the clinical outcome prediction. In the case of independent daily n-fractionated schedules, the function G in (Eq. 10) degenerates into $1/n$ [29], leading to the second term in SF of (Eq. 1) in the classical LQ model.

BED for the LQRG model is then expressed as:

$$\mathrm{BED} = \left(D + \frac{\beta G(\tau_R) D^2}{\alpha} - \frac{\frac{1}{2}\sigma^2 G(\tau_S) D^2}{\alpha} - \frac{\ln 2(T - T_k)}{\alpha \tau_P}\right) \quad (11)$$

The relations between the generalized Lea–Catcheside function $G(\tau)$ and the recovery time constant τ for both schemes were computed using numerical integration method. Dose and volume of PTV were extracted from the dose–volume histograms (DVHs) of radiation plans. The clinical endpoint linked to the TCP for model fitting was the time dependent LPFS. The calculated TCP(t) is fitted to the measured LPFS(t), where t is the time from the start of radiotherapy to the time of follow up. The least chi-square method was utilized in the fitting [30]. The free parameters in the function were determined by minimizing the cost function, which was the mean absolute error, using a gradient descent method. The absolute and relative fitting errors for LPFS were calculated using formulas in Appendix A. The confidence intervals for estimated parameters were determined following standard procedures in nonlinear regression [31]. Akaike information criterion (AIC) was used to compare the quality of the models (see Appendix B). Leave-one-out cross validation based on the time-dependent LPFS samples was performed to compare the generalization capabilities of the models. To examine the model performance without the influence of redistribution and reoxygenation, a model excluding the two terms were assessed in Appendix C. All the aforementioned calculations in tumor control probability modeling were conducted on a cloud-based clinical data service platform OncoEvidance™ v1.0 (Homology Medical, Suzhou, China).

Results

Table 1 details the baseline characteristics and treatment-related parameters. Thirty-seven and twenty-one patients received Hyper- and Hypo-IMRT. The median chemotherapy cycles were four and six in total, and three and five prior to radiotherapy, respectively.

Tumor response

At first follow-up, there were 24 (64.9%) patients found with CR or PR, 11 (29.7%) with stable disease (SD) and 2 (5.4%) with progressive disease (PD) in the Hyper-IMRT group, while 11 (52.4%) with CR or PR, 6 (28.6%) with SD and 4 (19.0%) with PD in the Hypo-IMRT group ($p = 0.30$).

Local control and overall survival

At a median radiologic follow-up of 18 (2–53) and 16 (5–50) months in the Hyper- and Hypo-IMRT groups, 21 and 13 patients had local relapse. The most common sites in Hyper-IMRT group were the ipsilateral hemithorax and regional lymph nodes (10/21, 47.6%), followed by nodes only (8/21, 38.1%) and the ipsilateral hemithorax only (3/21, 14.3%); while in the Hypo-IMRT group nodal recurrence (6/13, 46.1%) was found most frequently, followed by recurrence in the ipsilateral hemithorax (4/13, 30.8%) and in both sites (3/13, 23.1%). The 2-year LPFS rates of Hyper- and Hypo-IMRT patients were 34.1% and 27.9% ($p = 0.44$, Fig. 1A). In the Hyper-IMRT group, eleven recurrent cases were treated with chemotherapy, one with chest chemoradiotherapy, one with radioactive seed implantation, and eight not known. In the other group, six received palliative chemotherapy and others not record.

At a median clinical follow-up of 19 (2–53) and 16 (5–50) months, 12 and 7 deaths occurred. The 2-year OS was 76.9% *vs* 76.9% in Hyper- and Hypo-IMRT groups ($p = 0.26$, Fig. 1B).

None of the clinic-pathologic characteristics was statistically associated with LPFS or OS on univariate analysis (Supplementary Table 1).

Toxicities

Seven patients (18.9%) treated with Hyper-IMRT were found with grade 3–4 toxicities, including seven (18.9%) with grade 3 neutrocytopenia and two (5.4%) with grade 3 anemia. Eight (38.1%) in the Hypo-IMRT group presented grade 3–4 toxicities, including three (24.4%) grade 3–4 neutrocytopenia, three (14.3%) grade 3–4 thrombocytopenia, one (4.8%) grade 4 anemia and one (4.8%) grade 3 esophagitis. There was no statistical difference between the incidences of severe toxicities ($p = 0.13$).

Table 1
Baseline clinico-pathologic and treatment-related characteristics.

Characteristics	Hypo-IMRT		Hyper-IMRT		*p*
	No.	%	No.	%	
Sex					
Male	18	85.7	29	78.4	*0.73*
Female	3	14.3	8	21.6	
Age (years)					
<60	13	61.9	21	56.8	*0.79*
≥60	8	38.1	16	43.2	
T					
T1-2	4	19.0	9	24.3	*0.75*
T3-4	17	81.0	28	75.7	
N					
N1-2	9	42.9	22	59.5	*0.28*
N3	12	57.1	15	40.5	
M					
M1a	14	66.7	28	75.7	*0.55*
M1b	7	33.1	9	24.3	
Chemotherapy					
Concurrent	13	61.9	18	48.6	*0.42*
Sequential	8	38.1	19	51.4	
Cycles of chemotherapy					
<4	2	9.5	4	10.8	*0.64*
4–6	19	90.5	33	89.2	

Hypo-IMRT: hypofractionated intensity-modulated radiation therapy, Hyper-IMRT: hyperfractionated intensity-modulated radiation therapy.

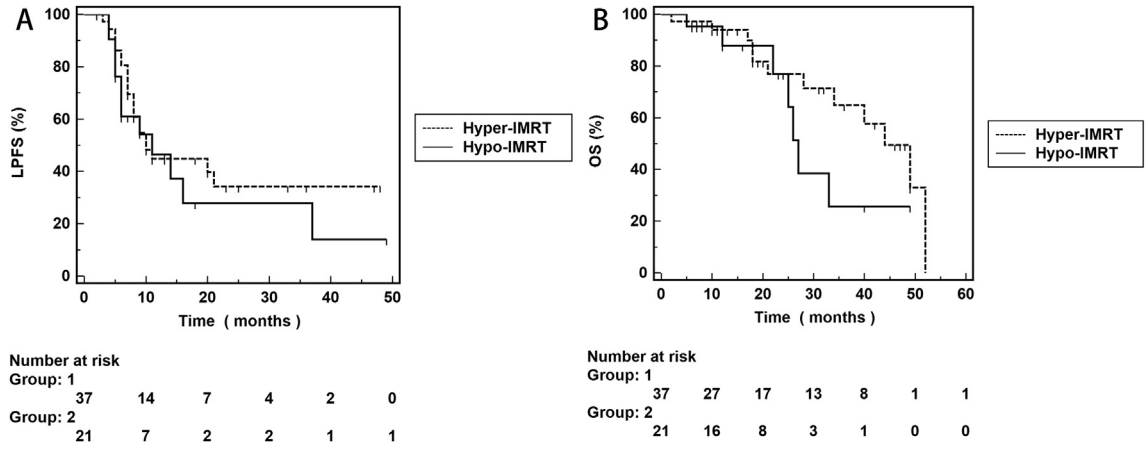

Fig. 1. (A) Local progression-free survival; (B) Overall survival. LPFS: local progression-free survival, Hyper-IMRT: hyperfractionated intensity-modulated radiation therapy, Hypo-IMRT: hypofractionated intensity-modulated radiation therapy, OS: overall survival.

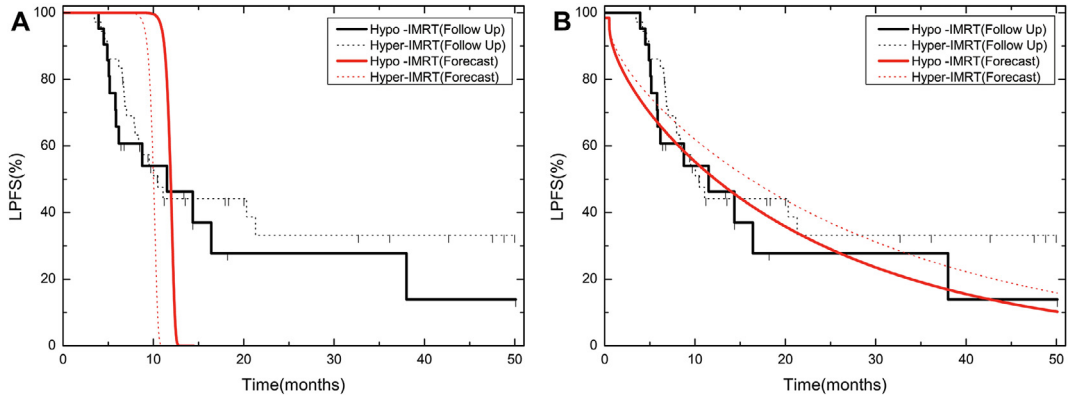

Fig. 2. Model fitting to LPFS data from the follow-up data with different dose fractionation schemes using (A) the classical LQ and TCP models, or (B) the new LQRG and TCP models. LPFS: local progression-free survival, LQ: linear-quadratic model, LQRG: LQ model incorporating cell repair, redistribution, reoxygenation, regrowth and Gompertzian tumor growth, Hypo-IMRT: hypofractionated intensity-modulated radiation therapy, Hyper-IMRT: hyperfractionated intensity-modulated radiation therapy.

Modeling

The mean total PTV doses were 45.4 and 44.6 Gy for Hyper-IMRT and Hypo-IMRT groups. The mean PTV volumes were 608.3 and 846.9 cm^3, respectively.

Fig. 2 presents the results of TCP (or LPFS) model fitting within a duration of 50 months. Compared with the excellent fit of the LQRG model, fitting of the LQ model failed immediately after 8 months. The average absolute and relative fitting errors for LPFS were 9.1% and 18.7% for Hyper-IMRT, and 8.8% and 16.2% for Hypo-IMRT of the new LQRG and TCP models, compared with 29.1% and 62.3% for Hyper-IMRT, and 30.7% and 65.3% for Hypo-IMRT of the classical LQ and TCP models. The values of model parameters and their confidence intervals are detailed in Table 2. Fig. 3 shows the BED–LPFS relation predicted at the 7th and 25th month, and suggests a better agreement between data and prediction in the LQRG model. Supplementary Table 2 lists the fitting errors of LQ model and LQRG model for the prediction of the relation between BED and LPFS at the 7th month and the 25th month.

Supplementary Table 3 lists the intermediate results of the calculation of LPFS at the end of the treatment. These intermediate items were extracted from the exponent part of the SF from both models. Supplementary Fig. 1 shows the relation between the generalized Lea–Catcheside function $G(\tau)$ and the recovery time constant τ for both schemes. Table 3 presents the metrics characterizing the quality of the LQ and the LQRG models.

As presented in Appendix C, when the redistribution and reoxygenation terms are excluded, the resulting model still yielded a much better fit than the classical LQ-based TCP model (AIC = −58.2), but was inferior to the LQRG model (AIC = −80.7).

Discussion

The OS and LPFS rates of the Hyper- and Hypo-IMRT groups were similar. It seemed that tumor control of the split fractionation (1.5 Gy, twice-daily) was comparable to that of combined fractionation (3 Gy, once-daily), probably due to the equivalent shortened treatment time. The selection of either schedule in extensive stage SCLC is reasonable. Hypofractioned radiotherapy was reported by several previous studies. Grønberg et al. compared 45 Gy/30 -fractions/twice-daily with 42 Gy/15 fractions/once-daily in limited stage SCLC. The study revealed more complete responses, but a trend toward higher local recurrence rate in the twice-daily arm. The survival time was 6.3 months longer in these patients but without statistical significance. The authors drew no firm conclusion and proposed a phase 3 clinical trial [6]. In a single-arm phase 2 trial evaluating the 55 Gy/22 fractions/once-daily scheme, the 2-year local control rate (76.4%) and 2-year OS (58.2%) were satisfactory [7]. Another retrospective study addressed that the scheme of 40 Gy/15 fractions/once-daily might result in similar median relapse-free survival time (12 *vs* 12 months) and 5-year overall

Table 2
Parameter values.

Parameter	LQ	LQRG	
		Value	95% CI
ρ (cm^{-3})	1.76×10^8	9.79×10^8	[0.73×10^8, 13.70×10^8]
α (Gy^{-1})	0.983	0.281	[0.276, 0.291]
β (Gy^{-2})	0.0962	0.0304	[0.0286, 0.0322]
σ^2 (Gy^{-2})	/	0.102	[0.097, 0.108]
τ_R (hour)	/	2.45	[1.22, 3.45]
τ_S (hour)	/	9.89	[8.42, $+\infty$)
τ_P (hour)	186.4	120.5	[104.5, 188.4]
T_k (hour)	369.0	10.5	(0, 161.0]
K_c	/	8.27×10^9	[7.62×10^9, 12.64×10^9]
σ_k	/	3.14×10^9	[1.86×10^9, 3.42×10^9]
δ	/	0.142	[0.132, 0.176]
α/β (Gy)*	10.2	9.2	[8.7, 9.9]

LQ: linear-quadratic model, LQRG: LQ model incorporating cell repair, redistribution, reoxygenation, regrowth and Gompertzian tumor growth, CI: confidence interval.
* Denotes the dependent variable.

survival (20% *vs* 25%) compared with 45 Gy/30 fractions/twice-daily scheme [32]. Therefore, the Hypo-IMRT scheme used in the current study deserves further exploration in clinical trials.

Calculated by the classical LQ model, the BED was 52.12 and 57.63 Gy for the Hyper- and Hypo-IMRT groups, inconsistent with the results from clinical observations. The fitting of LPFS from follow-up data failed as anticipated, thereby manifesting its incapability of TCP prediction. The LQRG and the new TCP model incorporated more potentially influential factors than its predecessors, reflected by the five terms in the SF formulation, which represents cell killing by one- or two-track actions (and possible repair), intercellular diversity of radiosensitivity and resensitization, delayed tumor regrowth and the Gompertzian tumor growth post-radiation, respectively. Moreover, a Gaussian distribution was adopted for the TCP modeling instead of the conventional Binomial/Poisson distribution. The tumor control criterion was more clinically reasonable in our study, that a lung tumor would be controlled for an individual patient if the number of tumor cells K was smaller than a critical number K_{cr}, rather than the requirement of killing all the tumor clonogens. The distribution of K followed a Gaussian distribution for the patient population.

An additional analysis of the intermediate results of the SF and BED revealed the main mechanisms behind the new models. First, the resensitization term, including redistribution and reoxygenation, made a positive difference between the two schemes. Second, the inclusion of the Gompertzian term and the reformulation of TCP with K_{cr} slowed down the rapid decaying rate of the LPFS as time proceeded on. Third, the characterization of the Lea–Catcheside function versus time constant variable revealed a gap between the two curves of the Lea–Catcheside function, representing the characteristic difference between the two schemes. This difference was embodied in the second and third term of the SF in (Eq. (9)) and subtly balanced by other factors to contribute to the final comparative clinical results. Therefore, the difference of

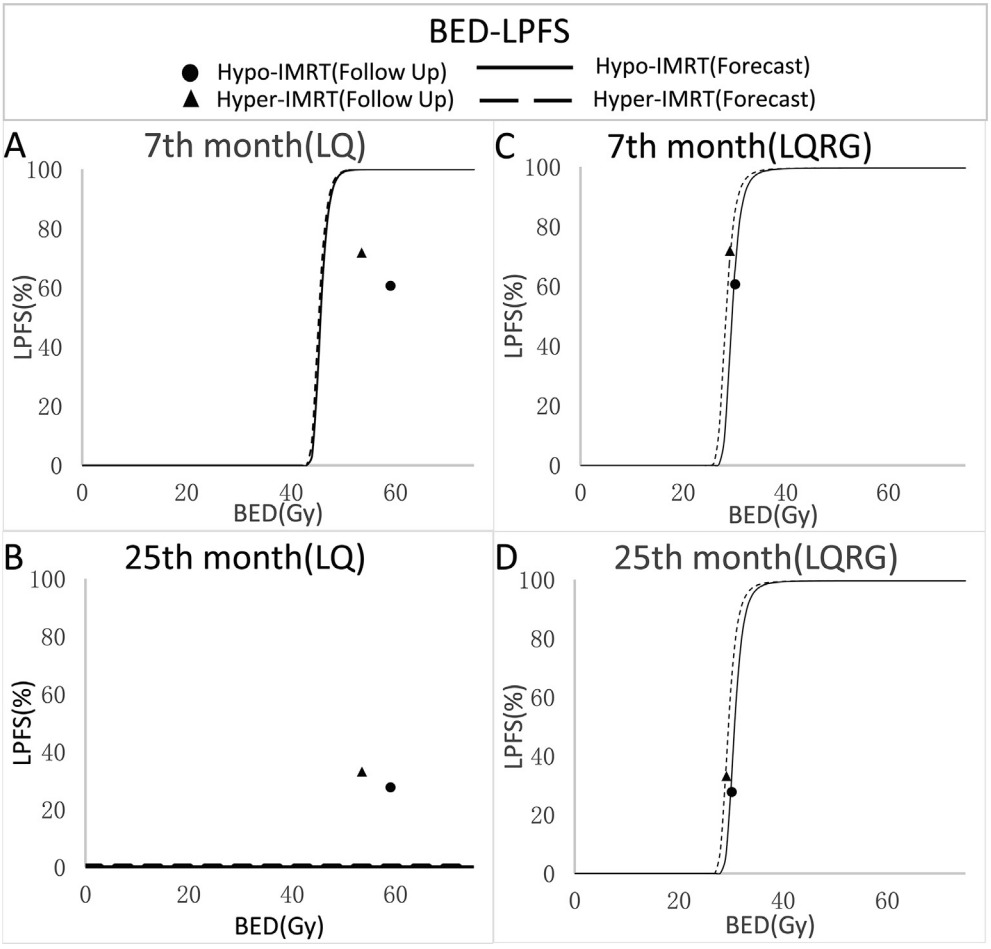

Fig. 3. Model fitting to the LPFS data versus BED. The classical LQ and TCP models fitting to LPFS data at (A) 7th month and at (B) 25th month. The new LQRG and TCP model fitting to LPFS data at (C) 7th month and at (D) 25th month. LPFS: local progression-free survival, BED: biological effective dose, LQ: linear-quadratic model, LQRG: LQ model incorporating cell repair, redistribution, reoxygenation, regrowth and Gompertzian tumor growth, Hypo-IMRT: hypofractionated intensity-modulated radiation therapy, Hyper-IMRT: hyperfractionated intensity-modulated radiation therapy.

Table 3
Model quality metrics.

	LQ	LQRG
Number of samples	58	58
Number of parameters	5	11
Maximum log likelihood	−15.4	51.4
Akaike information criterion	40.8	−80.7
Average prediction accuracy in leave-one-out cross validation (%)	38.2	83.6

LQ: linear-quadratic model, LQRG: LQ model incorporating cell repair, redistribution, reoxygenation, regrowth and Gompertzian tumor growth.

the BED of the LQRG model for the Hypo-IMRT and Hyper-IMRT is only 0.923 Gy, compatible with the follow up data. In addition, the mean PTV volume for the Hypo-IMRT group was slightly larger, which slightly lowered the height of LPFS curve for this group.

The preferred log likelihood and AIC of the LQRG model indicated its superior fitting accuracy and synthetic model quality. The 83.6% average prediction accuracy of leave-one-out cross validation for LQRG model demonstrates its sound predictive power and a better generalization capability. Compared to conventional LQ and TCP model, although six additional variables were added to the new models, the mechanistically driven nature of these variables could potentially interpret the outstanding balance between fitting accuracy and generalization capability. Besides, the model still showed better fit than the classical LQ-based TCP when excluding the redistribution and reoxygenation terms. We therefore conclude that the main reason for the superior model fit of the LQRG model is due to its form being Gaussian instead of binomial and inclusion of Gompertzian tumor regrowth. As to our knowledge, this is the first theoretical work to accurately predict the follow-up time dependence of LPFS for SCLC including correction for treatment duration, while previous publications only quantified the relation between LPFS and BED.

There was a trend toward higher incidence of severe toxicities in the Hypo-IMRT group, mainly in terms of hematologic toxicities, but without statistical difference due to limited sample size. It is hard to draw a solid conclusion since these patients also presented a greater number of chemotherapy cycles. Grønberg et al. addressed no differences in grade 3–4 neutropenic infections (37% *vs* 44%) between 45 Gy/30 fractions/twice-daily and 42 Gy/15 fractions/once-daily schemes. The incidences of grade 3–4 esophagitis were low in both groups in our study, in contrast to Turrisi et al.'s report, which indicated a rate of 27% with the utilization of conventional radiation technique [2]. In Grønberg et al.'s study using three-dimensional conformal radiotherapy, esophagitis was found in 33% and 31% of 45 Gy/30 fractions/twice-daily and 42 Gy/15 fractions/once-daily groups [6]. We explained the difference by our accurate radiation planning. Similarly, in CONVERT trial, the incidence of severe esophagitis between 45 Gy/twice-daily and 66 Gy/once-daily was similar, 19% and 19% [12]. The toxicities profile of hypofractionated radiotherapy needs to be further studied in matched cohort or clinical trials.

Our study is vulnerable to confounding factors due to its retrospective nature. Since there was no solid evidence favoring concurrent chemoradiotherapy in local control, patients with either concurrent or sequential chemoradiotherapy were included in this study, but there might still be potential bias. On the other hand, we reported a high local recurrence rate. There were several reasons. First, local failure was recorded until the last follow-up, not only at the first failure. Second, we only included highly selected patients and those with early disease progression were naturally excluded. Third, the time from the start of radiotherapy, but not the date of first-line treatment delivery, was used to calculate local control. However, although the local control rates were comparable, the overall survival curves tended to favor Hyper-IMRT in long-term follow-up. Our results should be further validated in external large cohorts.

Conclusions

The two fractionated radiation schemes, 45 Gy/30 fractions/twice-daily and 45 Gy/15 fractions/once-daily in the chest irradiation of extensive stage SCLC resulted in similar local control rates. The LQRG model is valuable in predicting the TCP (or LPFS) of the two schemes. We await the comparison of the schemes in a clinical trial.

Conflicts of interest

The authors declare no potential conflicts of interest.

Acknowledgement

This work was supported by the National Key R&D Program of China [Grant Number 2018YFC0116800].

Appendix A

Given a collection of independent and identically distributed observation points $\{(x_1,y_1),\ldots,(x_n,y_n)\}$, and a model described as $\tilde{y} = f(x)$, the average absolute and relative fitting errors for LPFS, i.e. MAE (mean absolute error) and MRE (mean relative error), are defined as follows.

$$\mathrm{MAE} = \frac{\sum_i \tilde{y}_i - y_i}{N}, \text{ and}$$

$$\mathrm{MRE} = \frac{\sum_i \left(\left|\tilde{y}_i - y_i\right|/y_i\right)}{N}$$

Appendix B

Given a collection of independent and identically distributed observation points $\{(x_1,y_1),\ldots,(x_n,y_n)\}$, the maximum likelihood of this observation is formulated as [32]:

$$\hat{L} = \max_{\theta\in\Theta} \prod_i P_{Y|X}(y_i|x_i;\theta) = \max_{\theta\in\Theta} \prod_i \frac{1}{\sqrt{2\pi\sigma^2}} \exp\left\{-\frac{[y_i - f(x_i;\theta)]^2}{2\sigma^2}\right\}$$

where $f(x;\theta) = y - \varepsilon$ denotes the fitting function with the parameter θ and the probabilistic distribution model for the noise ε is Gaussian with variance σ^2. If the fitting function is of k independent variables, the variance can be estimated as follows:

$$\sigma^2 = \frac{1}{n-k}\sum_{i=1}^{n}(y_i - f(x_i;\theta))^2.$$

Therefore, the log likelihood takes the following form:

$$\begin{aligned}\ln\left(\hat{L}\right) &= \max_{\theta\in\Theta}\sum_i \ln P_{Y|X}(y_i|x_i;\theta)\\ &= \min_{\theta\in\Theta}\sum_i\left\{\frac{[y_i - f(x_i;\theta)]^2}{2\sigma^2} + \frac{1}{2}\ln(2\pi\sigma^2)\right\}\\ &= \min_{\theta\in\Theta}\left\{\frac{n-k}{2} + \frac{n}{2}\ln(2\pi\sigma^2)\right\}\end{aligned}$$

Then the Akaike information criterion [33] is formulated as:

$$\mathrm{AIC} = 2k - 2\ln\left(\hat{L}\right)$$

where k is the number of model parameters.

Appendix C

To elucidate the role of the resensitization to the BED or LPFS, LQG, a reduced model of the LQRG, is also formulated by taking away the third term (including redistribution and reoxygenation) from the exponent of SF in the LQRG model. The model name "LQG" stands for the Linear Quadratic model with Gompertzian tumor growth. In the LQG, the SF and BED are then expressed respectively as:

$$\mathrm{SF} = \exp\left(-\alpha D - \beta G(\tau_R) D^2 + \ln 2 \frac{T - T_k}{\tau_P} + \left(\ln 2 \frac{\Gamma}{\tau_P}\right)^{\delta}\right)$$

and

$$\mathrm{BED} = \left(D + \frac{\beta G(\tau_R) D^2}{\alpha} - \frac{\ln 2 (T - T_k)}{\alpha \tau_P}\right)$$

The average absolute and relative fitting errors for LPFS are 9.1% and 18.5% for Hyper-IMRT and 9.7% and 20.3% for Hypo-IMRT of LQG and its relevant TCP model. Supplementary Fig. 2 shows the results of LQG-based TCP model fitting. Supplementary Tables 4–6 present the parameter values, model quality metrics and intermediate results calculated based on the LQG model.

The relevant results showed that tLQG had a little bit inferior model fitting and model generalization capabilities when compared to those of LQRG; but it also achieved much superior results when compared to those of LQ. This inferred that the good performance of LQRG could be largely contributed to the effect of Gompertzian growth and the Gaussian distribution used in the TCP modeling. However, after a close examination of the curves in Supplementary Fig. 2, it was manifested that the LQG model could not explain the slightly higher LPFS for the Hyper-IMRT group than the Hypo-IMRT group; while as manifested in Fig. 2B, LQRG successfully explained this phenomenon. Demonstrated in Supplementary Tables 3 and 6, the BED difference between Hypo-IMRT and Hyper-IMRT groups for LQG model is still too large, compared to that of LQRG, to reverse the height of the LFPS curves for both groups, even after taking into account the slightly larger average tumor volume and slightly lower average dose of the Hypo-IMRT group. These observations showed that although the effect of resensitization was relatively small compared to that of Gompertzian growth and the Gaussian distribution used in the TCP modeling, it would yet play a critical role in accurately interpreting the clinical LPFS results.

Appendix D. Supplementary data

Supplementary data to this article can be found online at https://doi.org/10.1016/j.radonc.2019.03.035.

References

[1] Lee KJ, Lee EJ, Hur GY, et al. The start of chemotherapy until the end of radiotherapy in patients with limited-stage small cell lung cancer. Korean J Intern Med 2013;28:449–55.
[2] Turrisi AT, Kim K, Blum R, et al. Twice-daily compared with once-daily thoracic radiotherapy in limited small-cell lung cancer treated concurrently with cisplatin and etoposide. N Engl J Med 1999;340:265–71.
[3] Chun SG, Hu C, Choy H, et al. Impact of Intensity-Modulated Radiation Therapy Technique for Locally Advanced Non-Small-Cell Lung Cancer: A Secondary Analysis of the NRG Oncology RTOG 0617 Randomized Clinical Trial. J Clin Oncolm 2017;35:56–62.
[4] Korreman SS. Image-guided radiotherapy and motion management in lung cancer. Br J Radiol 2015;88:20150100.
[5] Caillet V, Booth JT, Keall P. IGRT and motion management during lung SBRT delivery. Phys Med 2017;44:113–22.
[6] Grønberg BH, Halvorsen TO, Fløtten Ø, et al. Randomized phase II trial comparing twice daily hyperfractionated with once daily hypofractionated thoracic radiotherapy in limited disease small cell lung cancer. Acta Oncol 2016;55:591–7.
[7] Xia B, Hong LZ, Cai XW, et al. Phase 2 study of accelerated hypofractionated thoracic radiation therapy and concurrent chemotherapy in patients with limited-stage small-cell lung cancer. Int J Radiat Oncol Biol Phys 2015;91:517–23.
[8] Jeremic B, Shibamoto Y, Nikolic N, et al. Role of radiation therapy in the combined-modality treatment of patients with extensive disease small-cell lung cancer (ED SCLC): a randomized study. J Clin Oncol 1999;17:2092–9.
[9] Withers HR, Thames HD, Peters LJ. A new isoeffect curve for change in dose per fraction. Radiother Oncol 1983;1:187–91.
[10] Sachs RK, Brenner DJ. The mechanistic basis of the linear-quadratic formalism. Med Phys 1998;25:2071–3.
[11] Sachs RK, Hlatky LR, Hahnfeldt P. Simple ODE models of tumour growth and anti-angiogenic or radiation treatment. Mathl Comput Model 2001;33:1297–305.
[12] Faivre-Finn C, Snee M, Ashcroft L, et al. Concurrent once-daily versus twice-daily chemoradiotherapy in patients with limited-stage small-cell lung cancer (CONVERT): an open-label, phase 3, randomised, superiority trial. Lancet Oncol 2017;18:1116–25.
[13] Fowler JF. The linear-quadratic formula and progress in fractionated radiotherapy. Br J Radiol 1989;62:679–84.
[14] Fowler JF. Development of radiobiology for oncology-a personal view. Phys Med Biol 2006;51:R263–86.
[15] O'Donoghue JA. The response of tumours with gompertzian growth characteristics to fractionated radiotherapy. Int J Radiat Biol 1997;72:325–39.
[16] Wheldon EG, Lindsay KA, Wheldon TE. The dose–response relationship for cancer incidence in a two-stage radiation carcinogenesis model incorporating cellular repopulation. Int J Radiat Biol 2000;76:699–710.
[17] Lindsay KA, Wheldon EG, Deehan C, Wheldon TE. Radiation carcinogenesis modelling for risk of treatment-related second tumours following radiotherapy. Br J Radiol 2001;74:529–36.
[18] McAneney H, O'Rourke SF. Investigation of various growth mechanisms of solid tumour growth within the linear-quadratic model for radiotherapy. Phys Med Biol 2007;52:1039–54.
[19] Liu F, Tai A, Lee P, et al. Tumor control probability modeling for stereotactic body radiation therapy of early-stage lung cancer using multiple bio-physical models. Radiother Oncol 2017;122:286–94.
[20] Brenner DJ, Hlatky LR, Hahnfeldt PJ, Hall EJ, Sachs RK. A convenient extension of the linear-quadratic model to include redistribution and reoxygenation. Int J Radiat Oncol Biol Phys 1995;32:379–90.
[21] Horas JA, Olguin OR, Rizzotto MG. On the surviving fraction in irradiated multicellular tumour spheroids: calculation of overall radiosensitivity parameters, influence of hypoxia and volume effects. Phys Med Biol 2005;50:1689–701.
[22] Titz B, Jeraj R. An imaging-based tumour growth and treatment response model: investigating the effect of tumour oxygenation on radiation therapy response. Phys Med Biol 2008;53:4471–88.
[23] Tai A, Liu F, Gore E, Li XA. An analysis of tumor control probability of stereotactic body radiation therapy for lung cancer with a regrowth model. Phys Med Biol 2016;61:3903–13.
[24] Trotti A, Colevas AD, Setser A, et al. CTCAE v3. 0: development of a comprehensive grading system for the adverse effects of cancer treatment. Semin Radiat Oncol 2003;13:176–81.
[25] Lee SP, Leu MY, Smarthers JB, McBride WH, Parker RG, Withers HR. Biologically effective dose distribution based on Linear Quadratic model and its clinical relevance. Int J Radiat Oncol Biol Phys 1995;33:375–89.
[26] Lea DE. Actions of radiations on living cells. London: Cambridge University Press; 1946.
[27] Speer JF, Petrosky VE, Retsky MW, Wardwell RH. A stochastic numerical model of breast cancer growth that simulates clinical data. Cancer Res 1984;44:4124–30.
[28] Thames Jr HD, Peters LJ, Withers HR, Fletcher GH. Accelerated fractionation vs hyperfractionation: rationales for several treatments per day. Int J Radiat Oncol Biol Phys 1983;9:127–38.
[29] O'Rourke SF, McAneney H, Hillen T. Linear quadratic and tumour control probability modelling in external beam radiotherapy. Math Biol 2009;58:799–817.
[30] Moraru IC, Tai A, Erickson B, Li XA. Radiation dose responses for chemoradiation therapy of pancreatic cancer: an analysis of compiled clinical data using biophysical models. Pract Radiat Oncol 2014;4:13–9.
[31] Bates DM, Watts DG. Nonlinear regression analysis and its applications. John Wiley & Sons Inc; 1988.
[32] Bettington CS, Tripcony L, Bryant G, Hickey B, Pratt G, Fay M. A retrospective analysis of survival outcomes for two different radiotherapy fractionation schedules given in the same overall time for limited stage small cell lung cancer. J Med Imaging Radiat Oncol 2013;57:105–12.
[33] Akaike H. A new look at the statistical model identification. IEEE T Automat Contr 1974;19(6):716–23.